

REPORTS



Novel chimeric monoclonal antibodies that block fentanyl effects and alter fentanyl biodistribution in mice

Bhupal Ban^{a†}, Rodell C. Barrientos^{b,c§}, Therese Oertel^b, Essie Komla^{b,c}, Connor Whalen^b, Megan Sopko^a, Yingjian You^a, Partha Banerjee^a, Agnieszka Sulima^d, Arthur E. Jacobson^d, Kenner C. Rice^d, Gary R. Matyas^b, and Vidadi Yusibov^{aE}

^a Pharmaceutical Center, Indiana Biosciences Research Institute, Indianapolis, Indiana, United States; ^bLaboratory of Adjuvant and Antigen Research, U.S. Military HIV Research Program, Walter Reed Army Institute of Research, Silver Spring, Maryland, United States; ^c U.S. Military HIV Research Program, Henry M. Jackson Foundation for the Advancement of Military Medicine, Bethesda, Maryland, United States; ^dDepartment of Health and Human Services, Drug Design and Synthesis Section, Molecular Targets and Medications Discovery Branch, Intramural Research Program, National Institute on Drug Abuse and the National Institute on Alcohol Abuse and Alcoholism, National Institutes of Health, Bethesda, Maryland, United States

ABSTRACT

The prevalence and societal impact of opioid use disorder (OUD) is an acknowledged public health crisis that is further aggravated by the current pandemic. One of the devastating consequences of OUD is opioid overdose deaths. While multiple medications are now available to treat OUD, given the prevalence and societal burden, additional well-tolerated and effective therapies are still needed. To this point, we have developed chimeric monoclonal antibodies (mAb) that will specifically complex with fentanyl and its analogs in the periphery, thereby preventing them from reaching the central nervous system. Additionally, mAb-based passive immunotherapy offers a high degree of specificity to drugs of abuse and does not interfere with an individual's ability to use any of the medications used to treat OUD. We hypothesized that sequestering fentanyl and its analogs in the periphery will mitigate their negative effects on the brain and peripheral organs. This study is the first report of chimeric mAb against fentanyl and its analogs. We have discovered, engineered the chimeric versions, and identified the selectivity of these antibodies, through *in vitro* characterization and *in vivo* animal challenge studies. Two mAb candidates with very high (0.1–1.3 nM) binding affinities to fentanyl and its analogs were found to be effective in engaging fentanyl in the periphery and blocking its effects in challenged animals. Results presented in this work constitute a major contribution in the field of novel therapeutics targeting OUD.

ARTICLE HISTORY

Received 6 June 2021
Revised 5 October 2021
Accepted 6 October 2021

KEYWORDS

Fentanyl mAb; passive immunization; opioid use disorder; opioids; fentanyl analogs

Introduction

Data from a recent Centers for Disease Control and Prevention (CDC) report revealed that 67,000 deaths due to drug overdose occurred during the 12-month period ending April 2019.¹ Overdose deaths due to heroin have increased at a rate of 10% a year from 2005 to 2010, then by 33% per year from 2010 to 2014, and by 19% from 2014 to 2016. The most dramatic increase in deaths was due to synthetic opioids, such as illicitly manufactured fentanyl and its analogs (IMF), which have increased 88% per year from 2013 to 2016, with a 2016 death rate of 6.2 per 100,000. From January to February 2017, 90% of the accidental overdose deaths in Ohio were attributed to IMF.² A steep increase in the use of IMF alone or as additive to heroin continues to rise.^{3–5} Furthermore, IMF overdose is reported to be acute and rapid, requiring multiple doses of intranasal naloxone.³ The abuse of synthetic opioids has also led to an increased risk of acquiring an infectious disease such as the human immune deficiency virus (HIV) due to needle sharing.^{6,7} Finally, with the mounting annual cost of ~\$78.5 billion, in the United

States,⁸ incurred by the opioid epidemic, novel and pragmatic approaches are urgently needed to address this public health burden.

Limited treatment modalities remain a major barrier toward the successful mitigation of opioid use disorder (OUD). There are four pharmacotherapies currently approved to treat OUD: methadone, buprenorphine, naloxone and naltrexone. Oral buprenorphine/naloxone combinations (e.g., SUBOXONE®) are the most widely used treatment for relapse prevention, and recently, sustained-release injections of buprenorphine have been approved. The most dramatic impact on opioid overdose has been intranasal administration of the antagonist naloxone, which rapidly reverses opioid overdose.³ While opioid overdose can be reversed by naloxone, its use poses several challenges: 1) multiple doses may be required to reverse the effects of synthetic fentanyl analogs;^{9,10} 2) the limited time window for efficacy upon overdose, which may not always be practical; and 3) it precipitates opioid withdrawal symptoms.^{9–11}

CONTACT Gary R. Matyas  gmatyas@hivresearch.org  Laboratory of Adjuvant and Antigen Research, U.S. Military HIV Research Program, Walter Reed Army Institute of Research, Silver Spring, Maryland 20910, United States

[†]Present Address: Entrada Therapeutics, 6 Tide St., Boston, Massachusetts, 02210, United States

[§]Present Address: Merck & Co., Inc., 126 E. Lincoln Avenue, Rahway, New Jersey, 07065, United States

^EPresent Address: Biomedical Advanced Research and Development Authority (BARDA), 200 Independence Avenue, SW, Washington, D.C. 20201, United States

 Supplemental data for this article can be accessed on the [publisher's website](#).

© 2021 Taylor & Francis Group, LLC

This is an Open Access article distributed under the terms of the Creative Commons Attribution-NonCommercial License (<http://creativecommons.org/licenses/by-nc/4.0/>), which permits unrestricted non-commercial use, distribution, and reproduction in any medium, provided the original work is properly cited.

Current research efforts are focused on developing alternatives or complementary modalities to the four approved products. An alternative approach to treat substance use disorders is use of vaccines or biologics that target specific drugs of abuse (DoA). Although the proof-of-concept for vaccines against DoA was demonstrated over 40 years ago,^{12,13} it has taken decades for the use of vaccines to treat SUDs to gain momentum. In the early 1970s, seminal efforts were devoted to hapten design that mimicked morphine, methamphetamine, and nicotine. These haptens, primarily, were used to generate antibodies for the detection of DoA. This area of research waned by the 1980s, but, over the past 15–20 years, interest in drug-specific antibodies resurfaced. As such, continued efforts to improve hapten design have led to vaccine candidates that can induce effective antibodies.^{14,15} When the DoA enters the bloodstream, these antibodies bind the drug and impede it from crossing the blood–brain barrier, thereby preventing it from interacting with its molecular target (e.g., the μ -opioid receptor) in the central nervous system (CNS).

For a vaccine directed at an abused substance to be effective, it must induce high titer, high affinity, and long-duration antibodies. There have been multiple Phase 1 and Phase 2 clinical trials demonstrating the safety and efficacy of vaccines to DoA.^{16–22} The best-studied vaccine for a DoA is against nicotine. However, Phase 3 clinical trials failed to meet the study primary endpoint of volunteer cessation of smoking,²³ although post-hoc analysis detected higher cessation rates in participants with the highest antibody titers.^{23,24} Similar findings were found in a Phase 3 clinical trial for cocaine.²⁵ Thus, the data from the cocaine and nicotine vaccine trials indicated that a significant subset of patients did not produce a sufficient antibody response for clinical efficacy, limiting the practicality of vaccine approach for general use. Clearly, there is a threshold antibody concentration, which may differ for each substance of abuse, required to curb habitual use of an abused substance. More recently, studies in animals have shown that the fentanyl vaccine-induced antibodies cross-reacting with multiple fentanyl analogs, including carfentanil,^{26–28} which have been found in IMF.²⁹ Although this is promising data, the antibody titer induced by the fentanyl vaccine dropped rapidly following immunization.^{27,30,31}

Decades of vaccine research, preclinical and clinical, point to the potential role antibodies could play in addressing OUD. There is an emerging body of evidence supporting the potential of monoclonal antibodies (mAbs) as a therapeutic modality for OUD. For example, recent publications show that mAbs directed at fentanyl and related molecules can sequester large amounts of drug in the periphery and reduce biodistribution to the brain, suggesting these mAbs could be used as a treatment modality for OUD.^{32,33} The preclinical studies strengthen the potential utility of mAbs as a viable treatment modality for OUD that would greatly benefit from proof-of-concept studies in humans.

Like a vaccine, passive immunotherapy with a mAb is based on complexing a DoA in the periphery, thereby preventing it from reaching the CNS. This approach offers a high degree of specificity to a DoA, can be administered in quantities to sustain amounts required for clinical efficacy in all patients, and does not interfere with an individual's ability to use any of

the medications currently used to treat OUDs. Moreover, for those individuals who are immunosuppressed, including those with HIV/AIDS or autoimmune conditions, a mAb-based passive immunotherapy would be preferred approach. Finally, unlike a vaccine, a mAb-based approach offers immediate 'protection' against the DoA, whereas it may take weeks or months to produce sufficient antibody titers with a vaccine.

A large number of overdose deaths are due to fentanyl, primarily due to presence of trace amount of fentanyl and its analogs in the heroin supply.^{34–36} In pursuit of a suitable anti-fentanyl mAb, we produced two candidates, P1C3H9 and P1B6H7. The mAbs were derived from mice immunized with a novel fentanyl vaccine reported by Barrientos, *et al.*³⁷ The *in vitro* characterization and *in vivo* studies of these mAbs revealed very high (0.1–1.3 nM) binding affinities to fentanyl and selected analogs. The mAb candidates were effective in binding fentanyl in the periphery and blocking the translocation of the drugs to the brain, which resulted in negating the anti-nociceptive effects of the drug in challenged animals.

Results

Recombinant antibody generation, expression, and characterization

We recently reported an efficacious vaccine candidate against fentanyl in mice.³⁷ This vaccine, called TT-*para*-AmFenHap/ALF43A, (Figure 1a) elicited a high titer of drug-specific antibodies that cross-reacted with fentanyl, fentanyl analogs, but not with drugs used for OUD therapy. We exploited the same animal model to develop the chimeric mAbs described in this study. Each chimeric mAb is composed of the constant domain of human IgG and the variable domains derived from mouse IgG. Female Balb/c mice were immunized with TT-*para*-AmFenHap/ALF43A vaccine and collected splenocytes were used to generate hybridoma clones. The experimental strategy is depicted in Figure 1b. P1B6H7 and P1C3H9 hybridoma candidates, based on their binding properties and specificity, were selected for further studies. The cDNAs from these clones were synthesized using random hexamers and PCR amplification using the respective V and J gene-specific forward and reverse primers with 15-bp overlap at 5' and 3' ends, including restriction sites (Supplementary Table S1). The resulting PCR products, variable domains of heavy (VH) and light (VL) chains, were cloned into linear vectors containing the human IgG1, and Ig κ constant region genes using in-fusion cloning kits, respectively. The P1B6H7 and P1C3H9 sequences were analyzed using the Kabat database of VH and VL sequences; the variable region sequences are shown in Table 2 and Supplementary Table S3.³⁸ The recombinant chimeric antibodies VL and VH genes belonged to mouse IgG V subgroups, including J and D gene segments as shown in Supplemental Table S2. Recombinant chimeric antibodies were transiently expressed in Chinese hamster ovary (CHO) cells, purified using protein A affinity chromatography as shown in Figure 2a, and further characterized by enzyme-linked immunosorbent assay (ELISA) (Figure 2b). The mAbs reacted with BSA-*para*-AmFenHap in an ELISA, but did not react with BSA-SM(PEG)₂.

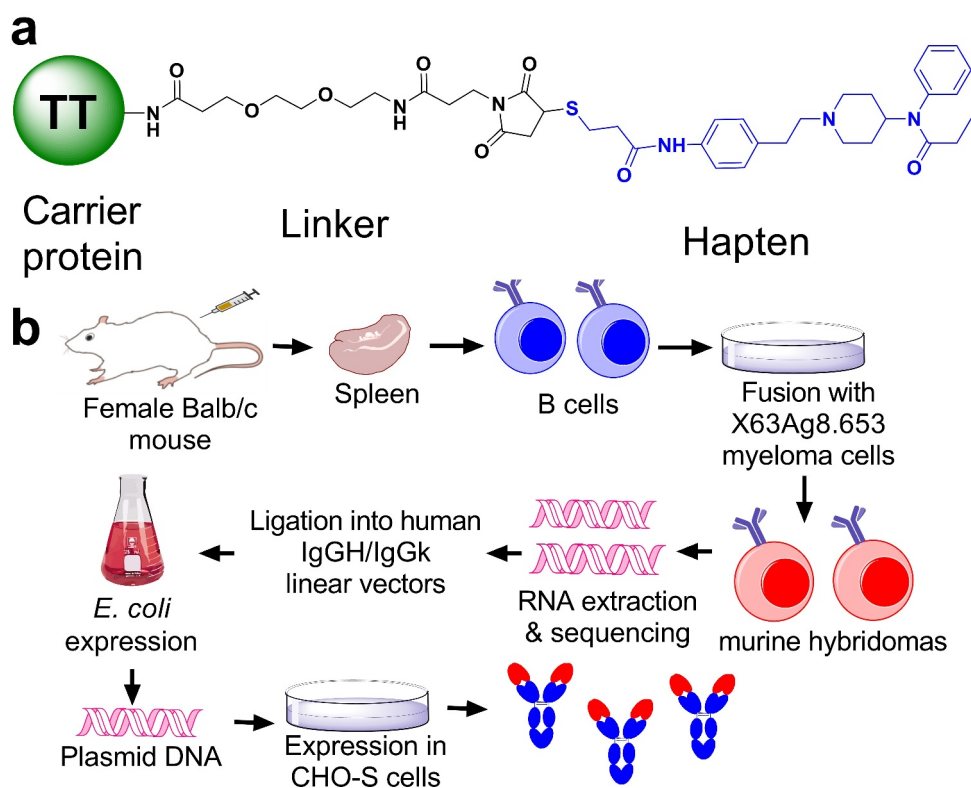


Figure 1. Description of immunogen and experimental strategy. a) Design of the fentanyl vaccine that was used to immunize mice. The immunogen is composed of tetanus toxoid (TT) carrier protein conjugated to the *para*-AmFenHap hapten through the NHS-PEG₂-maleimide linker. b) Experimental strategy to generate the chimeric mAb described in this study. The constant IgG domains in the chimeric mAbs originated from human IgG while the variable domains were from mouse.

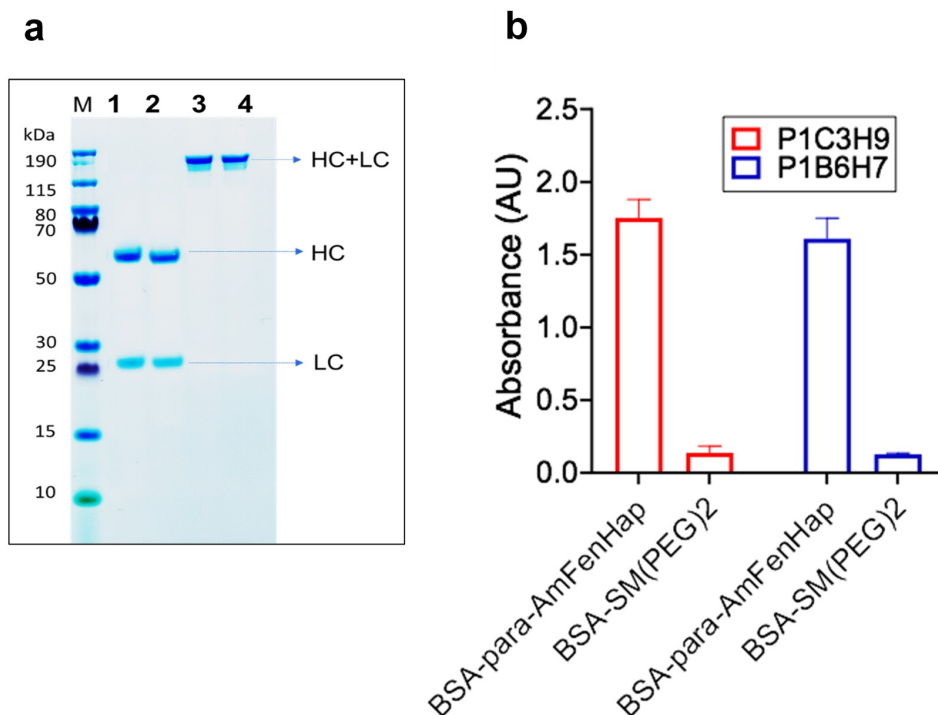


Figure 2. Characterization of purified mAb. a) SDS-PAGE analysis of purified anti-fentanyl chimeric antibodies. Purification of anti-fentanyl antibodies using protein A affinity chromatography. Lane M represents molecular marker, lane 1 represents P1B6H7 Ab under reduced condition, and lane 2 represents P1C3H9 Ab under reduced condition, respectively. Lanes 3 and 4 represent P1B6H7 and P1C3H9 Abs under non-reducing condition, respectively. HC indicates heavy chain and LC indicates light chain. b) Confirmatory ELISA of chimeric version of anti-fentanyl antibodies derived from hybridomas.

Drug binding and cross-reactivity

We assessed whether the mAb candidates are able to sequester fentanyl and analogs *in vitro* using equilibrium dialysis-liquid chromatography-tandem mass spectrometry (ED-LC-MS/MS).³⁷ Both mAb candidates P1C3H9 and P1B6H7 effectively bound fentanyl at 6.7 nM concentration of either mAb (Figure 3a). The 50% fractional bound fentanyl were at 1:3200 dilution of the stock, corresponding to ~0.2 nM mAb. The antibody-drug dissociation constants (K_d) were in the nanomolar range (Table 1). We also tested other fentanyl analogs acryl fentanyl, cyclopropyl fentanyl, and furanyl fentanyl, and obtained a similar trend using their respective EC_{50} values (Figure 3b-d). The EC_{50} corresponds to the mAb concentration that effectively bound 50% of the drug used in the assay. A low EC_{50} suggests a relatively higher affinity to the assayed drug.

To determine if recombinant antibodies are cross-reactive with drugs used for OUD therapy, we tested the binding against methadone, naltrexone, buprenorphine, and naloxone using ED-LC-MS/MS.³⁷ Results showed that neither mAb had significant binding to these four drugs (fraction bound <0.25) (Figure 3e-h).

Molecular modeling of the antigen-binding domain of anti-fentanyl mAb

We next investigated the molecular interactions of fentanyl with the two mAb candidates *in silico*. Sequence alignment for P1B6H7 and P1C3H9 antibody variable regions shows the heavy chains are 42% identical and light chains are 52.47% identical, respectively. The homologues modeling structures of the murine P1B6H7 and P1C3H9 (IgG1/ κ) antigen-binding domains were generated using the Chemical Computing Group MOE software.

The canonical structure designation of the complementarity-determining regions (CDR) loops was based upon the length of the loops and the presence of key residues at specific locations in the antibody sequence. The structural alignment (Figure 4a) clearly indicated that the structure of these antibodies does not perfectly overlap, and structural differences are in the loop regions, including CDRs. LCDR1 in P1C3H9 is 5 residues longer than its counterpart in P1B6H7 (Table 2). The two antibodies bind the fentanyl ligand in dramatically different modes (Fig. S1). The energy of the final model was determined to be -3,546.84 kJ/mol for P1B6H7 and -3,816.92 kJ/mol for P1C3H9, for the fully minimized energy structures, and the root-mean-square deviation (RMSD) between the fully minimized structure and the initial model was 0.27 Å using all backbone atoms. In P1B6H7, the binding site was almost completely buried with the tip of its benzyl moiety facing solvent. In P1C3H9, the binding site was a groove, and it appears to rely on overall surface complementarity. The ligand interacting residues for the loops shown in Figure 4(b,c) are summarized in Table S5.

While all CDR loops are involved in forming the binding site of P1B6H7 antibody (Figure 4b), only five CDR loops are involved in formation the binding site of P1C3H9 (Figure 4c), with CDRL2 providing no direct contact to the ligand. The

molecular structures of the fentanyl ligands bound to the two antibodies are remarkably similar (RMSD value 0.631 Å). A cationic ligand was involved in cation- π interactions with the antibody aromatic side chain, which may increase its binding affinity. The typical nonpolar hydrogen- π interactions are the interactions between hydrogen atoms, attached to carbon atoms, and the conjugate π -systems. In the case of P1B6H7, an aspartic acid (Asp H¹⁰¹) residue of the carboxyl group interacted with the carbon 1 position of fentanyl using a hydrogen donor. Fentanyl ligand's first nitrogen atom interacts with the π -cloud of the aromatic ring of tyrosine (Tyr L⁹¹) in a cationic- π interaction, as do the fentanyl ligand's carbon 2 and 4 (C4 and C8) hydrogen atoms interaction Tyr L⁹¹ as shown Figure 4d and Fig. S2. In the case of P1C3H9, fentanyl ligand's nitrogen atom interacts with the π -cloud of the aromatic ring of tyrosine (Tyr H^{102c}) in cationic- π interaction. The fentanyl ligand's carbon 4 (C4) hydrogen atom interacts with the π -cloud of the aromatic ring of tyrosine (Tyr H¹⁰²ⁱ) through nonpolar hydrogen- π interaction. Similarly, fentanyl ligand's aromatic ring π -cloud interacts with Tyr H¹⁰²ⁱ carbon's hydrogen and hydroxyl (OH) group through nonpolar π -hydrogen interaction, as shown in Figure 4e and Fig. S2.

Efficacy assessment and fentanyl biodistribution *in vivo*

The efficacy of CHO-cell produced and purified mAbs was assessed using tail immersion after a single fentanyl challenge dose (0.1 mg/kg, subcutaneous (s.c.)). We found that mice intravenously (i.v.) administered 1.0 mg of either mAb were significantly protected against fentanyl-induced antinociception as measured using a tail immersion assay 15 mins post-fentanyl dosing (Figure 5). The control group exhibited the antinociceptive effects of fentanyl administration.

Immediately after the antinociception test, blood and brain were collected for fentanyl analysis using LC-MS/MS. In mice administered mAbs P1B6H7 and P1C3H9, fentanyl levels in the blood were significantly higher (by ~20-fold) compared to control (Figure 6a). An opposite trend was observed in the brain (Figure 6b), where the mAb recipients had significantly lower (~3-fold) fentanyl concentration in the brain compared to controls.

Discussion

Pragmatic approaches are needed to mitigate OUD, particularly in the context of fentanyl abuse and overdose. Our research has addressed this public health burden by identifying anti-fentanyl mAbs that can neutralize both fentanyl and some of its highly potent analogs, and block fentanyl activity in a preclinical model. In particular, we generated chimeric mAbs P1C3H9 and P1B6H7 and determined that 1) these mAbs bound fentanyl and fentanyl analogs (cyclopropyl fentanyl, acryl fentanyl, and furanyl fentanyl), but not drugs used for opioid abuse therapy (naloxone, naltrexone, methadone, or buprenorphine); 2) passive immunization protected mice from antinociceptive effects of fentanyl; and 3) both mAbs effectively sequestered fentanyl in the blood and prevented access to the brain.

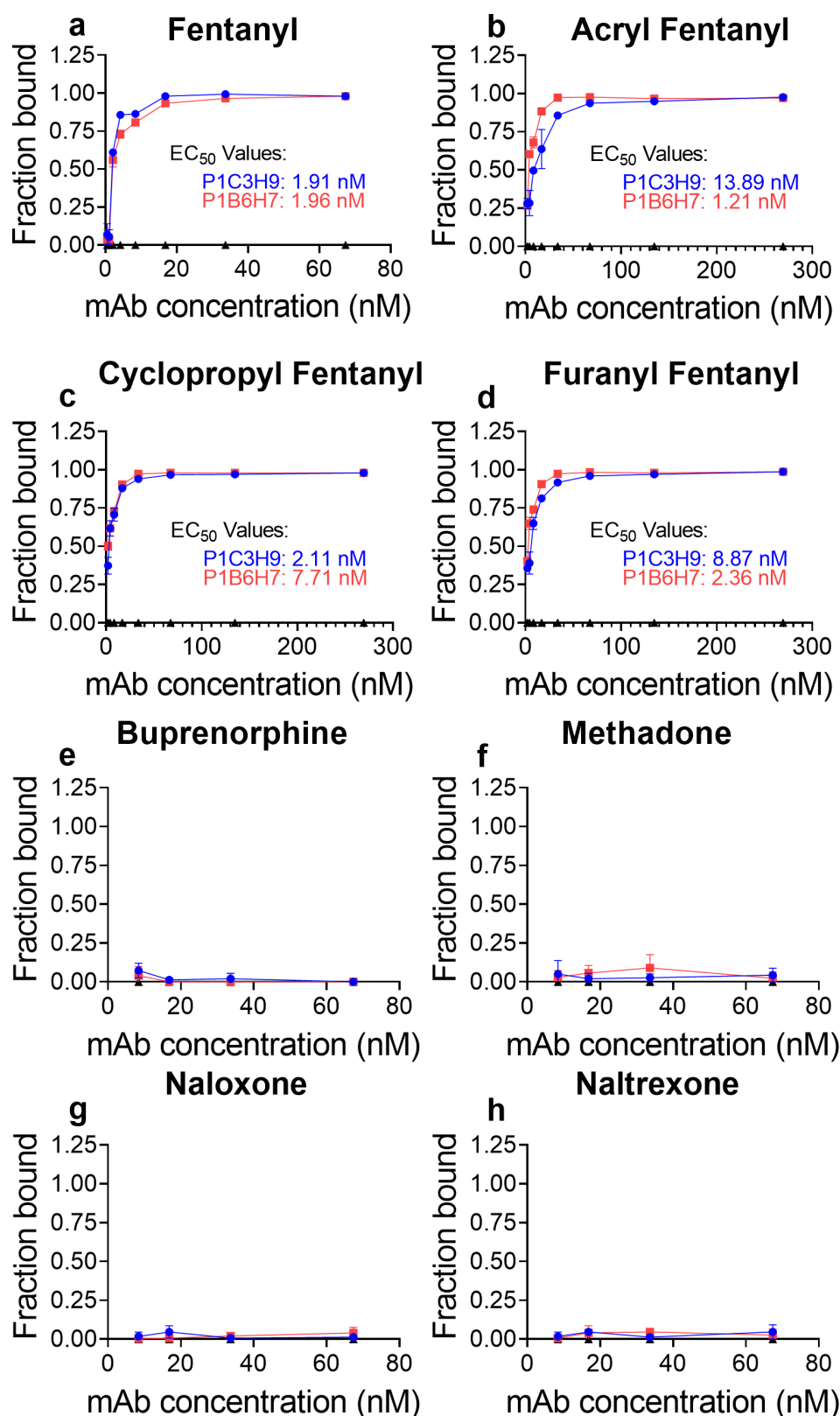


Figure 3. Specificity and cross-reactivity of mAb. Stock mAb solutions in PBS (1.0 mg/mL) were diluted with a buffer that contained 5 nM of indicated drugs and dialyzed against buffer in an equilibrium dialysis plate. Drug concentrations in the sample and buffer chambers were determined after 24 h, and fraction bound was calculated. a) fentanyl, b) acryl fentanyl, c) cyclopropyl fentanyl, d) furanyl fentanyl, e) buprenorphine, f) methadone, g) naloxone, h) naltrexone. Data shown are mean \pm std dev of triplicate measurements. Red: mAb P1C3H9, Blue: mAb P1B6H7.

Table 1. Antibody-drug dissociation constants (K_d) of chimeric mAb.

Drug target	Antibody affinity (K_d), nM	
	P1C3H9	P1B6H7
Fentanyl	0.15 ± 0.03	1.28 ± 0.12

Table 2. Amino acid sequences were deduced from DNA sequences and CDRs were selected as described in Kabat database.

		P1C3H9	P1B6H7
Light chain	CDR1	KASQNVGNNVA	RSSKSLLRNGITYLY
	CDR2	SASYRYS	QMSNLAS
	CDR3	QQYNSYPFT	AQNLELPWT
Heavy chain	CDR1	SSVMH	SGYWN
	CDR2	NINPYNDGTYNEKFKG	YISYSGSTYYNPSLKS
	CDR3	EGIYYGSSYRDY	YPYNGHNGYLDY

This study is the first report on chimeric mAbs that target fentanyl and its analogs. Opioid-targeting murine mAbs have been previously reported and found efficacious in animal models.^{32,33,39} In our work, the clones P1C3H9 and P1B6H7 were formed by the human constant domains and mouse

variable domains. Mouse mAbs are not ideally suited for clinical use because they are typically immunogenic. Thus, human patients may generate antibodies that neutralize the mouse mAbs, making chronic antibody treatment ineffective. MABs that contain human sequence, such as chimeric, humanized, or fully human mAbs, are more desirable for therapeutic purposes.

In silico molecular docking showed that the binding sites of these two antibodies have strikingly different topologies. As expected for a small antigen, the P1B6H7 binding site is a deep pocket that buries most of the ligand surface upon interaction. The fentanyl binding site of P1C3H9 can be described rather as a shallow depression on the protein surface, a topology that is considered to be more appropriate for larger antigens such as peptides. This change in binding site topology is due to conformational rearrangements of CDR loops and can therefore be directly attributed to their sequence differences.

The drastic difference in the overall topology of binding sites (pocket versus groove) allows P1B6H7 to bury a larger part of the ligand. This energetic deficiency due to electrostatic

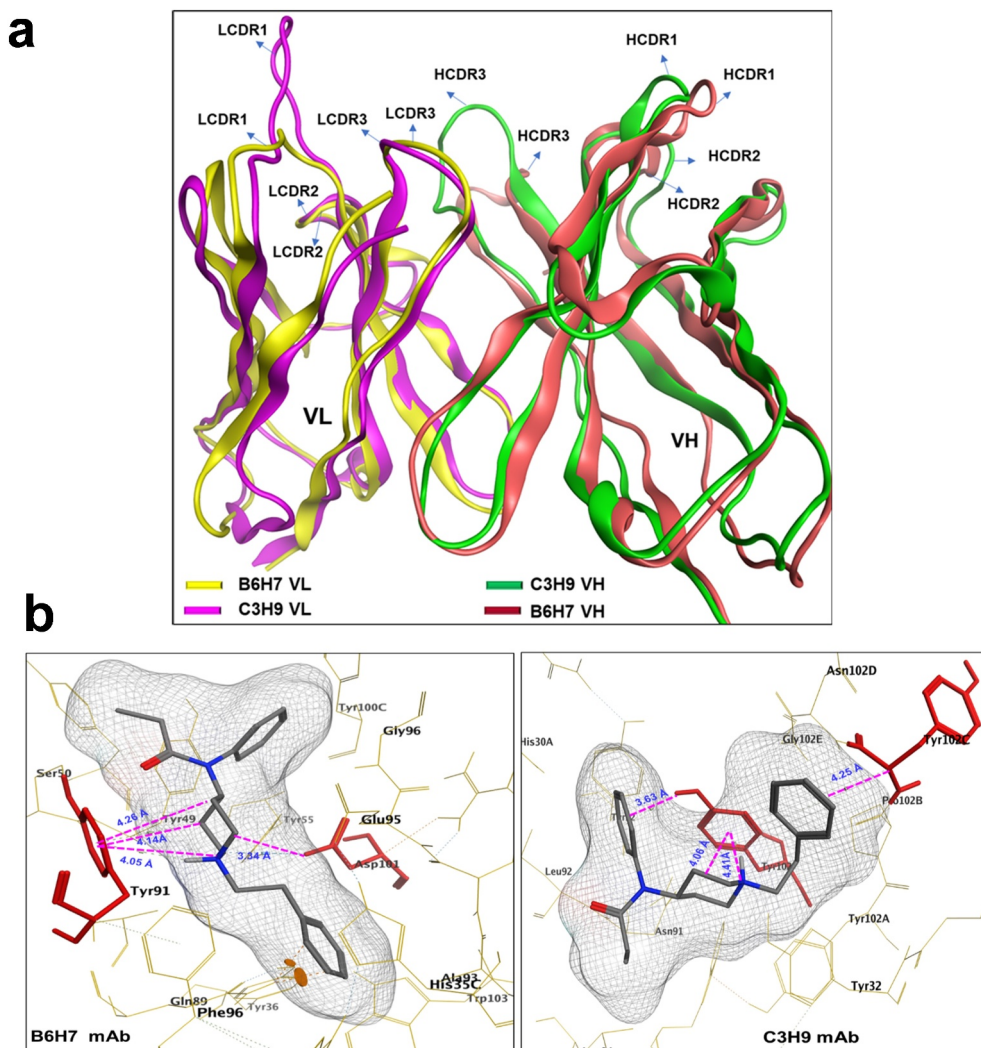


Figure 4. Molecular modeling of mAbs and their interaction with the fentanyl ligand. a) Predicted 3-dimensional (3D) structures alignment of the variable domain of antibodies B6H7 and C3H9 single-chain variable fragments (scFvs) with a comparison of the binding pockets. P1B6H7 is yellow (VL) and dark red (VH). P1C3H9 is purple (VL) and green (VH). The CDRs are indicated using arrow mark, L1CDR represents for light chain and H1CDR represents for heavy chain, respectively. b) The residues forming binding sites with fentanyl ligand (gray black) of antibodies: P1B6H7 and P1C3H9. The elements of specific protein-ligand interactions are shown. The key residues of mAbs interact with fentanyl ligand are shown in red.

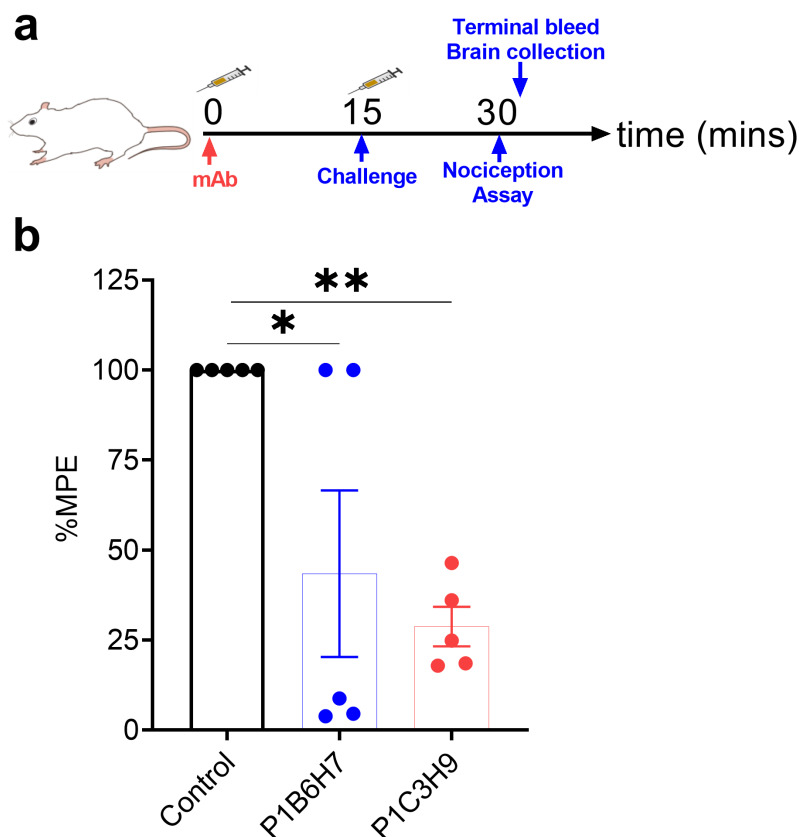


Figure 5. Effect of mAb on the fentanyl-induced antinociception. Mice ($n = 5\text{--}7/\text{group}$) were immunized with 1.0 mg of indicated mAb (i.v.) and challenged with 0.1 mg/kg fentanyl (s.c.). Controls did not receive mAb. Antinociception was measured 15 mins post-fentanyl using a tail immersion test. The percentage maximum possible effect (%MPE) was calculated as the posttest latency minus the pretest latency divided by the maximum time (10 seconds) minus the pretest latency times 100. Data shown are mean \pm s.e.m. Statistical analysis used ordinary one-way ANOVA with Bonferroni correction for multiple comparisons. * $p < .001$, ** $p < .01$. Red: mAb P1C3H9, Blue: mAb P1B6H7, Black: Control.

interactions in the P1C3H9-fentanyl complex is compensated by a stacking interaction between the fentanyl phenyl ring motifs and tyrosine (Tyr H^{102I}), the interaction lacking in the P1B6H7-antibody complex. This compensation lowers the binding energy levels (Table S6), directly from the electrostatic interaction between π -electron clouds and from improved van der Waals interactions between protein and piperidine and phenyl moieties of the fentanyl ligand. Both antibodies use water-mediated hydrogen bonding and cation- π interaction between the nitrogen atom of fentanyl and a nearby tyrosine residues in both antibodies, and these should contribute equally to their binding affinity. It is important to note that in each case the interactions are with different parts of the antibody and that this does not appear to relate to activity or efficacy. One interesting conclusion drawn from our analysis of the two binding sites is that hydrophobic interactions contribute similarly to their respective binding affinities.

It is well understood that protein-protein recognition may be achieved in diverse ways, because of the vast number of possible epitopes in large antigens. It is also well understood that protein-protein recognition sites are large enough to provide high affinity via various sets of interactions. It is expected, however, that for progressively smaller ligands recognition may converge to a unique mode because the binding site must encompass the entire ligand and the number of potential antigenic determinants is reduced. Hence, the conclusion may be drawn that even small

ligands that have a limited number of recognition determinants can bind to structurally diverse binding sites with comparable affinities.

Our mAb candidates bound to fentanyl and analogs with high affinity. We measured the affinities of P1C3H9 and P1B6H7 using ED-LC-MS/MS and found that the fentanyl K_d values (0.15 ± 0.03 and 1.28 ± 0.12 nM, respectively) are similar to the competitive IC₅₀ of the lead 6A4 mAb reported by Smith *et al.*³² that had $\sim 10^{-11}$ M affinity and the mAb HY4-1F9 clone reported by Baehr *et al.*,³³ which had <2 nM. These affinity values, however, cannot be directly compared because different techniques were used to measure them. Nevertheless, the mAb candidates have been shown to bind tightly to target drugs. Strong binding mAb are desirable because they can be given at lower doses and still abrogate opioid effects.³³ Both mAb P1C3H9 and P1B6H7 cross-reacted with potent fentanyl analogs acryl fentanyl, cyclopropyl fentanyl, and furanyl fentanyl, which have modifications at the N-acyl moiety (Figure 3a-d). These analogs have similar or at least three-fold higher potency than fentanyl and have been found in postmortem specimens from opioid overdose victims.⁴⁰⁻⁴³

It is important that candidate therapeutics do not impede existing medications to OUD. The mAb candidates described here are not cross-reactive with OUD medications. Using ED-LC-MS/MS, we showed that mAb P1C3H9 and P1B6H7 did not bind methadone, buprenorphine, naloxone, and naltrexone (Figure 3e-h). These findings are not surprising because the

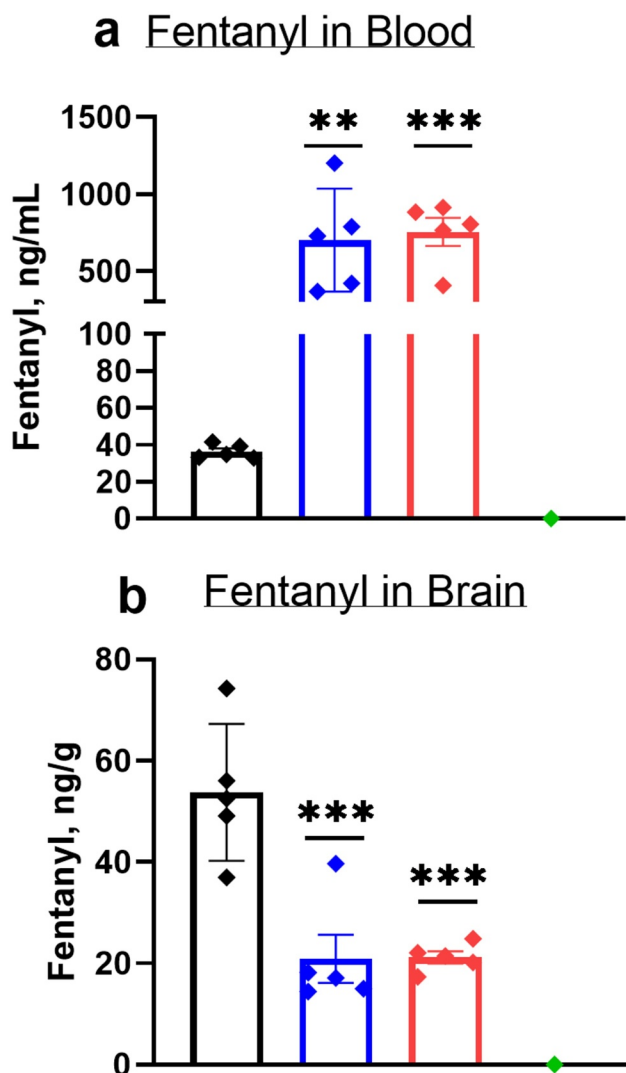


Figure 6. Blood-brain distribution of fentanyl in mice. Mice ($n = 5$ /group) were immunized with 1.0 mg of indicated mAb (*i.v.*) and challenged with 0.1 mg/kg fentanyl (*s.c.*). Controls (black bars) did not receive mAb. Mice were sacrificed and blood and brain were collected for fentanyl measurements using LC-MS/MS. Data shown are mean \pm std dev. Statistical analysis used ordinary one-way ANOVA with Bonferroni correction for multiple comparisons. ** $p < .001$, *** $p < .0001$. Red: mAb P1C3H9, Blue: mAb P1B6H7.

chemical structure of these drugs and the hapten used in the TT-*para*-AmFenHap vaccine are vastly different (Fig. S3).³⁷ In the active immunization model, mice antisera also did not cross-react to these drugs.³⁷ These results suggested that the mAbs presented here could be used in tandem with OUD medications for patients who are actively seeking therapy.

The mAb candidates protected mice from the antinociceptive effects of fentanyl. Mice that received 1.0 mg of the mAb P1C3H9 and P1B6H7 (~40 mg/kg, *i.v.*, 25 g mouse) 15 mins before challenge with 0.1 mg/kg fentanyl (*s.c.*) had significantly reduced antinociception than unimmunized control as measured using a tail immersion test. This test, which evaluates spinal reflex, is one of the standards used to assess the antinociceptive effects of opioids.^{37,44,45} Previous works have used intraperitoneal (*i.p.*) administration of mAb and *s.c.* drug challenges.³³ Typical protective mAb doses ranges from 30 to 120 mg/kg, with higher affinity mAb requiring lower dosing.^{32,33} A sublethal fentanyl challenge dose of 0.1 mg/kg is typically used in mouse models.^{33,37,46}

Predominantly, immunotherapeutics to drugs of abuse are believed to work by complexing the drugs in the periphery and preventing their access to the brain. We attempted to investigate this mechanism by challenging mice with fentanyl and quantify fentanyl concentrations in blood and brain. After the fentanyl challenge dose and antinociception measurement, mice were sacrificed, and blood and brain samples were immediately collected for fentanyl analysis. The mAb candidates altered the bio-distribution of fentanyl in mice. We found that the fentanyl concentration in the blood is higher than in the brain for mice that received the mAbs. This result suggests that fentanyl has been effectively sequestered in the blood and has in effect been blocked from reaching the brain. The reverse is true for mice that did not receive the mAbs: fentanyl concentration was higher in the brain than in the blood. These observations are consistent with our equilibrium dialysis experiments where these mAbs were found to bind the drugs *in vitro* (Figure 3). As such, it is prudent to assume that mAbs have complexed the drugs in the blood and prevented their access to the brain. Undoubtedly, much is needed to be learned on the mechanism of action of immunotherapeutics to drugs of abuse, a subject that remains a rich area for future research. This retention of fentanyl occurs because the mAb circulating in the periphery bind and trap free fentanyl immediately following *s.c.* administration. The blood-brain biodistribution measurements agree with the findings from the tail-immersion assay. Mice that had reduced fentanyl concentration in the brain and increased concentration in the blood had lower % Maximum Possible Effect (%MPE) compared to controls. Previous reports from the groups of Janda^{26,32} and Pravetoni^{33,46} on the analysis of fentanyl in blood and brain from either actively or passively immunized mice gave comparable results. In our study, mice were challenged with 0.1 mg/kg (*s.c.*) fentanyl. Mice are typically less sensitive to opioids compared to humans. The documented lethal dose for mice was ~ 4 mg/kg, while it is ~0.03 mg/kg in humans (~ 2 mg, 70 kg average human). Our study revealed that *in vivo*, a 1 mg *i.v.* dose of mAbs (~40 mg/kg, 25 g mouse) could bind and prevent 1/3 of the 0.1 mg/kg fentanyl from reaching the brain. In a real-world scenario where humans receive ~2 mg of fentanyl, and assuming other factors remain constant, a dose of ~40 mg/kg of mAb given prophylactically could prevent fatal overdose. The purpose of the mAbs is to act as a prophylactic and not an antidote to overdose in patients who relapse. Previous works from the groups of Janda^{26,32} and Pravetoni^{33,46} also tested the mAbs and vaccines as prophylactics rather than as antidotes. Fundamentally, it would be interesting to see the efficacy of these mAbs when considered as an antidote. Taken together, the data presented in this study indicate that mAbs P1B6H7 and P1C3H9 are highly effective in an *in vivo* mouse model and warrant further clinical development.

Materials and methods

Materials

Centricon filters were purchased from Amicon (Beverly, MA). Super Blue TMB Microwell Substrate was a product of KPL (Gaithersburg, MD). Microwell plates for ELISA (high-binding, flat bottom) and standard tissue culture plastic were purchased from Corning/Costar (Cambridge, MA). Ultralink

Bio-support beads (50–80 μm diameters) for equilibrium binding studies were purchased from SapidyneInc (Boise, ID). Horseradish peroxidase-labeled goat anti-human IgG were purchased from Jackson ImmunoResearch Laboratories (Catalog; AB_2337577, West Grove, PA). Fetal bovine serum (FBS) (low IgG) was from Hyclone Laboratories (Logan, UT). HEPES-buffered saline (HBS, 137 mM NaCl, 3 mM KCl, 10 mM HEPES, pH 7.4) was prepared using reagents from Fisher Scientific (Pittsburgh, PA). L-glutamine (Catalog; 25030149), Penicillin-Streptomycin (Catalog; 15140122) from Fisher Scientific, Pittsburgh, PA), and bovine serum albumin (BSA) (fraction V, metal-free (Catalog; 10735094001) from Sigma Aldrich Inc St. Louis, MO 68178.

Cell lines

The P1B6H7 and P1C3H9 hybridomas were grown in Dulbecco's Modified Eagle's Medium (DMEM) (Gibco BRL, USA) supplemented with 10% (v/v) FBS (Gibco BRL, USA), 100 U/ml penicillin (Gibco BRL, USA) and 100 $\mu\text{g}/\text{mL}$ streptomycin (Gibco BRL). ExpiCHO-S cells used for transient expression of antibody were obtained from Thermo Fisher Scientific (Waltham, MA) and cultured according to the manufacturer's protocol.

Immunizations and hybridoma generation

All animal studies were conducted under an approved animal use protocol in an Association for Assessment and Accreditation of Laboratory Animal Care International-accredited facility in compliance with the Animal Welfare Act and other federal statutes and regulations relating to animals. Experiments involving animals adhered to the principles stated in the Guide for the Care and Use of Laboratory Animals, 8th edition.⁴⁷ A previously described vaccine composed of a fentanyl hapten conjugated to tetanus toxoid (TT-*para*-AmFenHap) and adjuvanted with liposomes containing monophosphoryl lipid A adsorbed on aluminum hydroxide was used to immunize mice.³⁷ Female BALB/c mice ($n = 10$ per group) were immunized intramuscularly (*i.m.*) on weeks 0, 3, 6, and 14 using 50 μL of the vaccine formulation as described.³⁷ This dose contained 10 μg of TT-*para*-AmFenHap (based on the protein content of the protein-hapten conjugate), 20 μg of synthetic monophosphoryl 3-deacyl lipid A (3D-PHAD) in ALF43, and 30 μg of aluminum in aluminum hydroxide (Alhydrogel) in DPBS pH 7.4. ALF43 contained DMPC/DMPG/cholesterol/3D-PHAD at a molar ratio of 9:1:7.5:1.136; the molar ratio of phospholipids/3D-PHAD was 8.8:1.

Mice were boosted *i.v.* at week 38 with 10 μg TT-*para*-AmFenHap, 20 μg 3D-PHAD in ALF43, without Alhydrogel. Three days following the boost, mice were terminated, and spleens disaggregated into single-cell suspension in serum-containing culture media. B cells of the immunized mice were fused with nonproducing myeloma cells, namely X63Ag.653, using the ClonaCell-HY Hybridoma Kit (Stemcell Technologies). The fusion, selection and expansion were done following the experimental procedure of the kit. Once the fused hybridoma were appropriately expanded, the cells were selected based on the ability of cell culture media to bind BSA-*para*-AmFenHap in ELISA (Supplementary Figure S4) using the

method described previously.³⁷ The cells that bound in the assay were then selected and subcloned in HAT selection media to ensure that they were monoclonal. This resulted in two clones (P1B6H7 and P1C3H9) with isotype of mouse IgG1 heavy chain and kappa light chain.

Generation of recombinant chimeric antibodies, production, and purification

Total RNA was extracted from P1B6H7 and P1C3H9 hybridomas cells using QIAGEN's RNeasy Kit. cDNA was synthesized from RNA using SuperScript™ III First-Strand system for reverse transcription (RT)-PCR (Invitrogen CatLog: 8080051) according to the manufacturer's protocol using oligo (dT) and random hexamer primers. The variable region sequences of heavy-chain and light-chain genes were amplified from the cDNA using primer sets (Supplementary Table S1). PCR reactions were performed in a volume of 50 μL with 4 μL cDNA using Phusion® High-Fidelity PCR master Mix with HF Buffer (New England BioLabs, Ipswich, MA). The PCR reactions were carried out for 35 cycles, using annealing temperature (T_m) $58 \pm 2^\circ\text{C}$. The size of PCR products was verified by agarose gel electrophoresis. All primers used in Ig gene-specific PCRs included restriction sites (*AgeI* and *SalI* for IgGH, *AgeI* and *BsiWI* for Igk), which allowed direct cloning into expression vectors containing the human IgGH, IGK constant regions, respectively. Ligation of PCR-amplified variable regions of the heavy and light chains of P1B6H7 and P1C3H9 antibodies were performed using In-Fusion® HD Eco-Dry™ Cloning Kit (Takara Bio USA) fused into linear human IgG1/kappa vectors, respectively. Each ligation reaction was used to transform 50 μL of One Shot™ TOP10 Chemically Competent *E. coli* (Thermo Fisher Scientific, Waltham, MA). The transformed single bacterial colonies were used to re-amplify and isolate plasmid DNA, and subsequently clones were sequenced by Sanger sequencing. The sequences were assembled and assessed for translation into functional polypeptides using SnapGene 5.0.7 software and were analyzed in IMGT-VQUEST. Amino acid sequences predicted from the nucleic acid sequence were numbered and designated CDRs of light and heavy chain of isolated immunoglobulin genes were defined using VBASE2.

ExpiCHO-S cell (Thermo Fisher Scientific) were used for recombinant antibody expression. Transfection reactions were carried out using both correct sequenced variable region of heavy- and light-chain plasmid DNA with a 1:1 ratio 1 μg plasmid per 1 mL culture using an ExpiFectamine™ CHO Transfection Kit (Catalog; A29129, Thermo Fisher Scientific) including other supply reagents according to the manufacturer's instructions. The transfected cells incubated for an additional 3–6 days, at which time the conditioned medium was collected as recombinant chimeric antibodies (rchmAb) culture supernatant for analysis. The functionality of isolated VH/VL combination antibodies were validated by ELISA and Western analysis.

The chimeric IgG1/k antibodies were purified using a HiTrap™ MabSelect™ Prisma 5 mL column (Cytiva, Catalog; 17549852, MA) according to the manufacturer's protocol. Briefly, ExpiCHO-S cell culture supernatants were loaded on protein A agarose column to capture expressed IgG in the

medium, then washed with 20 mM sodium phosphate, 250 mM sodium chloride (NaCl), pH 7.4, followed by an additional wash with 20 mM sodium phosphate, pH 7.4, before elution with 100 mM sodium acetate, pH 3.5 and subsequently neutralized by 0.1 M Tris-HCl (pH 9.0). The purified IgG was further equilibrated in phosphate-buffered saline (PBS), pH 7.4 and concentrated using a Centricon centrifugal concentrator (30 KD MW cutoff, Fisher Scientific) at 4°C. Levels of endotoxin in each batch of purified antibody were determined to be <1 EU/mg of antibody measured by a LAL chromogenic quantitation kit (Thermo Scientific). The purified mAbs were subjected to matrix-assisted laser desorption/ionization time-of-flight mass spectrometry to determine molecular weight homogeneity and the presence of contaminating proteins (Supplementary Figure S5). High performance-size exclusion chromatography was also performed to assess aggregation states of the mAbs. Negligible aggregation was observed in the purified P1B6H7 and P1C3H9 that has been stored at -20°C for over 3 months of storage ((Supplementary Figure S6).

Drug binding and antibody affinity analysis

Drug binding was measured using ED-LC-MS/MS as described previously.⁴⁸ Briefly, mAbs were diluted with 0.05% BSA in DPBS, pH 7.4 (ED buffer) containing 5 nM of a drug. The following drugs were tested: fentanyl, cyclopropyl fentanyl, fentanyl, methadone, naloxone, buprenorphine, and methadone. An aliquot (100 µL) was seeded into sample chambers of the ED plate and the buffer chamber was filled with 300 µL of ED buffer. The plate was incubated at 4°C and 300 rpm for 24 h in a thermomixer. Aliquots (90 µL) from sample and buffer chambers were pipetted out and analyzed by LC-MS/MS. The detailed LC-MS/MS method has been previously described³⁷ and provided in Supplemental Methods (Tables S4 and S5).

Determination of K_d used competition ED as noted.⁴⁸ Briefly, mAb was diluted with 5 nM of isotopically labeled tracer drug (d_x where $x = 3$ or 5 heavy isotopes) in ED buffer at a serum dilution that yielded 50% binding in the serum-binding experiments. The buffer chambers were filled with ED buffer that contains an increasing concentration of competitor drug (final concentration, 0 nM to 40 nM). Half maximal inhibitory concentration (EC_{50}) was interpolated using four-parameter logistic curve (plot of % inhibition vs. concentration of competitive inhibitor). The % inhibition values were obtained using equation (3) and were used to calculate K_d .³⁷

Molecular modeling of the antigen-binding domain of anti-fentanyl mAb

The homologues modeling structures of the murine antibodies (IgG1/k) P1B6H7 and P1C3H9 single-chain variable fragments were generated using Chemical Computing Group MOE software (Chemical Computing Group ULC, Montreal Canada) and models were visualized with the program PyMoL (Schrödinger Inc., New York, New York). To understand the molecular interaction of fentanyl hapten ligand with the P1B6H7 and P1C3H9 antibodies, MOE software was used to analyze antigen-antibody docking.⁴⁹ The PDB structure of fentanyl ligand was obtained from the PubChem compound database. In this study, the

fentanyl ligand affinity score was obtained when ligand binds to antibody paratope. Furthermore, rigid, and induced fit (flexible) dockings were performed using the MOE software package. In MOE, all antibody structures were subjected to energy minimization using the CHARMM force field, and docking was performed with the 'Rigid Receptor' and 'Induced Fit' docking protocols. The docking was performed using the 'Triangle Matcher' placement method, which is the most efficient method for well-defined binding sites. All conformations per ligand were scored using the 'London dG' scoring function, submitted to a refinement step based on molecular mechanics and rescored with the 'GBVI/WSA dG' scoring function. GBVI/WSA dG, a force field-based scoring function, determines the binding free energy (kcal/mol) of the ligand from a given pose. In this study, the rotamer explorer RMSD limit was set to 2.0 Å, energy window to 4 kcal/mol and residues farther than 4.5 Å were kept fixed, and 10 ligand binding poses were ranked according to their CDOCKER energies. The electrostatic density of P1B6H7 and P1C3H9 antibodies and the binding pockets were predicted and visualized with the program MOE software. To predict the most critical binding contacts between the P1B6H7 and P1C3H9 antibodies and fentanyl ligand, Chemical Computing Group MOE software was used as described software method.⁴⁹

Passive transfer experiments in mice

Female BALB/c mice, 6–7 weeks of age received 1.0 mg of each test mAb by *i.v.* injection in the tail vein. Mice in the control group received saline. Thirty minutes after test mAb administration, animals received an *s.c.* fentanyl (0.1 mg/kg) challenge dose. This route has been used previously to evaluate anti-fentanyl vaccines.^{26,46} Antinociceptive effects were assessed 15 min after each fentanyl injection using tail immersion.^{44,50}

The tail-immersion assay involved immersing the mouse tail in a water bath set at 54°C. The latency times were measured with a cutoff time of 8 sec to prevent tail injury. Antinociception, measured as % Maximum Potential Effect (%MPE), was calculated using equation (1):

$$\%MPE = \frac{\text{Post fentanyl injection latency time} - \text{baseline latency time}}{\text{Cutoff latency} - \text{baseline latency time}} \times 100 \quad (1)$$

Analysis of fentanyl in blood and brain

The collected brain tissues were homogenized using a Benchmark Bead Bud 6 homogenizer. Samples were weighed in a tared 2 mL microcentrifuge tube with ceramic beads, then diluted with 2:1 ratio 1xDPBS. The tubes were then mixed at 6 m/s for 30 seconds, with a 30 second pause between each of the 3 cycles. The tubes were then transferred to a standard benchtop centrifuge and spun at 500 xg for 2 minutes, and homogenized brain samples were aspirated into clean 2 mL microcentrifuge tubes. Blood samples were prepared by standard benchtop centrifugation at 3100 xg for 3 minutes, and the resulting supernatant transferred to a new tube.

Samples were spiked with 10 µL of fentanyl- d_5 internal standard (100 ng/mL in methanol). Next, 100 µL of the respective samples were combined with LC-MS grade acetonitrile (3:1, vol:vol) and spun down at 9300 xg for 10 minutes at

4°C. Following centrifugation, the supernatant was collected in 18 × 150 mm glass tubes, and dried with nitrogen gas or air at 40–50°C. Samples were then reconstituted with 200 µL 1xDPBS and rapidly vortexed. Potential high abundant interferents in the sample such as phospholipids were eliminated using solid-phase extraction. Samples were applied to Bond Elute Plexa PCX cartridge and eluted by a fresh mixture of acetonitrile and ammonium hydroxide (95:5, vol:vol). The eluate was dried and reconstituted in 100 µL of 10 mM ammonium formate with 0.1% formic acid for LC-MS/MS analysis.

The resulting samples were then analyzed using a Waters Acquity UPLC system with Tandem Quadrupole Detector as previously described.³⁷ The detailed method is provided in Tables S4 and S5. The samples were run under the column conditions ACQUITY HSS T3, 2.1 × 100 mm, 1.8 µm at 65°C. The strong and weak wash were 90% acetonitrile in water and 10% methanol in water, respectively. The following mobile phases were used: Mobile phase A (10 mM ammonium formate with 0.1% formic acid) and mobile phase B (methanol with 0.1% formic acid). The instrument ran at a flow rate of 500 µL/minute, and injection volume of 10 µL, and 8.0 minutes per sample. Internal standard technique was used for quantification. The limit of quantification was 0.25 ng/mL fentanyl.

Data analysis

GraphPad Prism 8 (GraphPad Software, La Jolla, CA) was used for all statistical analyses and graphing of data. Ordinary one-way ANOVA with Bonferroni correction for multiple comparisons was used for statistical analysis of the blood–brain fentanyl distribution data. Differences were considered significant if $p \leq 0.05$. All values represent the mean ± standard error of the mean (SEM).

Acknowledgments

Research reported in this publication was supported by the National Institute on Drug Abuse of the National Institutes of Health under Award Number UG3DA048351 and by an Avant Garde award to GRM from NIDA (NIH grant no. 1DP1DA034787-01). The work of GRM, TO, EK, CW, and RCB was supported through a Cooperative Agreement Award (no. W81XWH-07-2-067) between the Henry M. Jackson Foundation for the Advancement of Military Medicine and the U.S. Army Medical Research and Materiel Command (MRMC). The work of AS, AEJ and KCR was supported by the NIH Intramural Research Program (IRP) of the National Institute on Drug Abuse and the National Institute of Alcohol Abuse and Alcoholism. The authors thank David McCurdy, Nadine Nehme, and Alexander Anderson for outstanding technical assistance. The authors also thank Dr. Marco Pravetoni and Jennifer R. Vigliaturo (University of Minnesota Medical School) for the hands-on training on the blood–brain drug distribution analysis.

Disclosure statement

This material has been reviewed by the Walter Reed Army Institute of Research, the National Institute on Drug Abuse, and Indiana Biosciences Research Institute. All animal studies were conducted under an approved animal use protocol in an Association for Assessment and Accreditation of Laboratory Animal Care International-accredited facility in compliance with the Animal Welfare Act and other federal statutes and regulations relating to animals. Experiments involving animals adhered to the principles stated in the Guide for the Care and Use of Laboratory Animals, 8th edition. There is no objection to its presentation and/or publication. The opinions or

assertions contained herein are the private views of the authors, and should not be construed as official, or as reflecting true views of the Department of the Army, the Department of Defense, NIDA, NIH or the US government. GRM, AS, KCR, and AEJ are inventors of a provision patent application filed by the Henry M. Jackson Foundation for the Advancement of Military Medicine (provisional patent Serial No.: 62/960,187; January 13, 2020).

Funding

This work was supported by the Henry M. Jackson Foundation [Cooperative Agreement Award No. W81XWH-07-2-067]; National Institute on Drug Abuse [Intramural Research Program]; National Institute on Drug Abuse [UG3DA048351, Avant Garde award 1DP1DA034787-01].

ORCID

Gary R. Matyas  <http://orcid.org/0000-0002-2074-2373>

References

1. National Vital Statistics System. 2019. Accessed: March 1, 2021. <https://www.cdc.gov/nchs/nvss/index.htm>
2. Daniulaityte RJM, Strayer K, Sizemore I, Harshbarger MD, Antonides HM, Carlson RR Overdose Deaths Related to Fentanyl and Its Analogs - Ohio, January-February 2017. *MMWR Morb Mortal Wkly Rep.* 2017; 66:904–08; doi:10.15585/mmwr.mm6638a8externalicon.
3. Somerville NJ, O'Donnell J, Gladden RM, Zibbell JE, Green TC, Younkin M, Ruiz S, Babakhanlou-Chase H, Chan M, Callis BP, et al. Characteristics of Fentanyl Overdose -Massachusetts, 2014–2016; *MMWR Morb Mortal Wkly Rep.* 2017; 66(14):382–86; doi:10.15585/mmwr.mm6614a2.
4. Carroll JJ, Marshall BDL, Rich JD, Green TC. Exposure to fentanyl-contaminated heroin and overdose risk among illicit opioid users in Rhode Island: a mixed methods study. *Int J Drug Policy.* 2017;46:136–45. doi:10.1016/j.drugpo.2017.05.023.
5. Macmadu A, Carroll JJ, Hadland SE, Green TC, Marshall BD. Prevalence and correlates of fentanyl-contaminated heroin exposure among young adults who use prescription opioids non-medically. *Addict Behav.* 2017;68:35–38. doi:10.1016/j.addbeh.2017.01.014.
6. Talu A, Rajaleid K, Abel-Ollo K, Rützel K, Rahu M, Rhodes T, Platt L, Bobrova N, Uusküla A. HIV infection and risk behaviour of primary fentanyl and amphetamine injectors in Tallinn, Estonia: implications for intervention. *Int J Drug Policy.* 2010;21(1):56–63. doi:10.1016/j.drugpo.2009.02.007.
7. Lambdin BH, Bluthenthal RN, Zibbell JE, Wenger L, Simpson K, Kral AH. Associations between perceived illicit fentanyl use and infectious disease risks among people who inject drugs. *Int J Drug Policy.* 2019;74:299–304. doi:10.1016/j.drugpo.2019.10.004.
8. Florence CS, Zhou C, Luo F, Xu L. The economic burden of prescription opioid overdose, abuse, and dependence in the United States, 2013. *Med Care.* 2016;54(10):901–06. doi:10.1097/MLR.0625.
9. Rzasz Lynn R, Galinkin JL. Naloxone dosage for opioid reversal: current evidence and clinical implications. *Ther Adv Drug Saf.* 2018;9(1):63–88. doi:10.1177/2042098617744161.
10. Moss RB, Carlo DJ. Higher doses of naloxone are needed in the synthetic opioid era. *Subst Abuse Treat Prev Policy.* 2019;14(1):6. doi:10.1186/s13011-019-0195-4.
11. Levine R, Veliz S, Singer D. Wooden chest syndrome: beware of opioid antagonists, not just agonists. *Am J Emerg Med.* 2020;38(2):411.e5–411.e6. doi:10.1016/j.ajem.2019.09.009.
12. Spector S, Parker CW. Morphine: radioimmunoassay. *Science.* 1970 12;168(3937):1347–48. doi:10.1126/science.168.3937.1347.
13. Bonese KF, Wainer BH, Fitch FW, Rothberg RM, Schuster CR. Changes in heroin self-administration by a rhesus monkey after morphine immunization. *Nature.* 1974;252(5485):708–10. doi:10.1038/252708a0.

14. Kosten TR, Domingo CB. Can you vaccinate against substance abuse? *Expert Opin Biol Ther.* 2013;13(8):1093–97. doi:10.1517/14712598.2013.791278.
15. Janda KD, Treweek JB. Vaccines targeting drugs of abuse: is the glass half-empty or half-full? *Nat Rev Immunol.* 2011;12(1):67–72. doi:10.1038/nri3130. PMID: 22173478.
16. Maurer P, Jennings GT, Willers J, Rohner F, Lindman Y, Roubicek K, Renner WA, Müller P, Bachmann MF. A therapeutic vaccine for nicotine dependence: preclinical efficacy, and Phase I safety and immunogenicity. *Eur J Immunol.* 2005;35(7):2031–40. doi:10.1002/eji.200526285.
17. Cornuz J, Zwahlen S, Jungi WF, Osterwalder J, Klingler K, van Melle G, Bangala Y, Guessous I, Müller P, Willers J, et al. A vaccine against nicotine for smoking cessation: a randomized controlled trial. *PLoS One.* 2008 Jun 25;3(6):e2547. doi:10.1371/journal.pone.0002547.
18. Cerny EH, Cerny T. Vaccines against nicotine. *Hum Vaccin.* 2009;5(4):200–05. doi:10.4161/hv.5.4.7310.
19. Hatsukami DK, Jorenby DE, Gonzales D, Rigotti NA, Glover ED, Oncken CA, Tashkin DP, Reus VI, Akhavan RC, Fahim RE, et al. Immunogenicity and smoking-cessation outcomes for a novel nicotine immunotherapeutic. *Clin Pharmacol Ther.* 2011;89(3):392–99. doi:10.1038/clpt.2010.317.
20. Hoogsteder PH, Kotz D, van Spiegel PI, Viechtbauer W, Brauer R, Kessler PD, Kalnik MW, Fahim RE, Van Schayck OC. The efficacy and safety of a nicotine conjugate vaccine (NicVAX®) or placebo co-administered with varenicline (Champix®) for smoking cessation: study protocol of a phase IIb, double blind, randomized, placebo-controlled trial. *BMC Public Health.* 2012;12(1):1052. doi:10.1186/1471-2458-12-1052.
21. Tonstad S, Heggen E, Giljam H, Lagerbäck PÅ, Tønnesen P, Wikingsson LD, Lindblom N, de Villiers S, Svensson TH, Fagerström KO. Nicotine®, a nicotine vaccine, for relapse prevention: a phase II, randomized, placebo-controlled, multicenter clinical trial. *Nicotine Tob Res.* 2013;15(9):1492–501. doi:10.1093/ntr/ntt003.
22. Hoogsteder PH, Kotz D, van Spiegel PI, Viechtbauer W, Van Schayck OC. Efficacy of the nicotine vaccine 3'-AmNic-rEPA (NicVAX) co-administered with varenicline and counselling for smoking cessation: a randomized placebo-controlled trial. *Addiction.* 2014;109(8):1252–59. doi:10.1111/add.12573.
23. Hartmann-Boyce J, Cahill K, Hatsukami D, Cornuz J. Nicotine vaccines for smoking cessation. *Cochrane Database Syst Rev.* 2012;2012(8):CD007072. doi:10.1002/14651858.CD007072.
24. Van Schayck OC, Horstman K, Vuurman E, De Wert G, Kotz D. Nicotine vaccination—does it have a future? *Addiction.* 2014;109(8):1223–25. doi:10.1111/add.12569.
25. Kosten TR, Domingo CB, Shorter D, Orson F, Green C, Somoza E, Sekerka R, Levin FR, Mariani JJ, Stitzer M, et al. Vaccine for cocaine dependence: a randomized double-blind placebo-controlled efficacy trial. *Drug Alcohol Depend.* 2014;140:42–47. doi:10.1016/j.drugalcdep.2014.04.003.
26. Bremer PT, Kimishima A, Schlosburg JE, Zhou B, Collins KC, Janda KD. Combatting synthetic designer opioids: a conjugate vaccine ablates lethal doses of fentanyl class drugs. *Angew Chem Int Ed Engl.* 2016;55(11):3772–75. doi:10.1002/anie.201511654.
27. Hwang CS, Smith LC, Natori Y, Ellis B, Zhou B, Janda KD. Efficacious Vaccine against Heroin Contaminated with Fentanyl. *ACS Chem Neurosci.* 2018;9(6):1269–75. doi:10.1021/acchemneuro.8b00079.
28. Hwang CS, Smith LC, Natori Y, Ellis B, Zhou B, Janda KD. Improved admixture vaccine of fentanyl and heroin hapten immunoconjugates: antinociceptive evaluation of fentanyl-contaminated heroin. *ACS Omega.* 2018;3(9):11537–43. doi:10.1021/acsomega.8b01478.
29. Strayer KE, Antonides HM, Juhascik MP, Daniulaityte R, Sizemore IE. LC-MS/MS-Based Method for the Multiplex Detection of 24 Fentanyl Analogues and Metabolites in Whole Blood at Sub ng mL⁻¹ Concentrations. *ACS Omega.* 2018;3(1):514–23. doi:10.1021/acsomega.7b01536.
30. Townsend EA, Blake S, Faunce KE, Hwang CS, Natori Y, Zhou B, Bremer PT, Janda KD, Banks ML. Conjugate vaccine produces long-lasting attenuation of fentanyl vs. food choice and blocks expression of opioid withdrawal-induced increases in fentanyl choice in rats. *Neuropsychopharmacology.* 2019;44(10):1681–89. doi:10.1038/s41386-019-0385-9.
31. Tenney RD, Blake S, Bremer PT, Zhou B, Hwang CS, Poklis JL, Janda KD, Banks ML. Vaccine blunts fentanyl potency in male rhesus monkeys. *Neuropharmacology.* 2019;158:107730. doi:10.1016/j.neuropharm.2019.107730.
32. Smith LC, Bremer PT, Hwang CS, Zhou B, Ellis B, Hixon MS, Janda KD. Monoclonal antibodies for combating synthetic opioid intoxication. *J Am Chem Soc.* 2019 Jul 3;141(26):10489–503. doi:10.1021/jacs.9b04872.
33. Baehr C, Kelcher AH, Khaimraj A, Reed DE, Pandit SG, AuCoin D, Averick S, Pravetoni M. Monoclonal antibodies counteract opioid-induced behavioral and toxic effects in mice and rats. *J Pharmacol Exp Ther.* 2020;375(3):469–77. doi:10.1124/jpet.120.000124.
34. Ciccarone D. Fentanyl in the US heroin supply: a rapidly changing risk environment. *Int J Drug Policy.* 2017;46:107–11. doi:10.1016/j.drugpo.2017.06.010.
35. Chandler RK, Villani J, Clarke T, McCance-Katz EF, Volkow ND. Addressing opioid overdose deaths: the vision for the HEALing communities study. *Drug Alcohol Depend.* 2020 Dec 1;217:108329. doi:10.1016/j.drugalcdep.2020.108329.
36. Frank RG, Pollack HA. Addressing the fentanyl threat to public health. *N Engl J Med.* 2017;376(7):605–07. doi:10.1056/NEJMp1615145.
37. Barrientos RC, Bow EW, Whalen C, Torres OB, Sulima A, Beck Z, Jacobson AE, Rice KC, Matyas GR. Novel vaccine that blunts fentanyl effects and sequesters ultrapotent fentanyl analogues. *Mol Pharm.* 2020;17(9):3447–60. doi:10.1021/acs.molpharmaceut.0c00497.
38. Al-Lazikani B, Lesk AM, Chothia C. Standard conformations for the canonical structures of immunoglobulins. *J Mol Biol.* 1997;273(4):927–48. doi:10.1006/jmbi.1997.1354.
39. Bogen IL, Boix F, Nerem E, Mørland J, Andersen JM. A monoclonal antibody specific for 6-monoacetylmorphine reduces acute heroin effects in mice. *J Pharmacol Exp Ther.* 2014;349(3):568–76. doi:10.1124/jpet.113.212035.
40. Fogarty MF, Papsun DM, Logan BK. Analysis of Fentanyl and 18 Novel Fentanyl Analogs and Metabolites by LC-MS-MS, and report of Fatalities Associated with Methoxyacetylfentanyl and Cyclopropylfentanyl. *J Anal Toxicol.* 2018;42(9):592–604. doi:10.1093/jat/bky035.
41. Concheiro M, Chesser R, Pardi J, Cooper G. Postmortem Toxicology of New Synthetic Opioids. *Front Pharmacol.* 2018;9:1210. doi:10.3389/fphar.2018.01210.
42. Drummer OH. Fatalities caused by novel opioids: a review. *Forensic Sci Res.* 2018 May 7;4(2):95–110. doi:10.1080/20961790.2018.1460063.
43. Wilde M, Pichini S, Pacifici R, Tagliabracchi A, Busardò FP, Auwärter V, Solimini R. Metabolic Pathways and Potencies of New Fentanyl Analogs. *Front Pharmacol.* 2019;10:238. doi:10.3389/fphar.2019.00238.
44. Le Bars D, Gozariu M, Cadden SW. Animal models of nociception. *Pharmacol Rev.* 2001;53(4):597–652. PMID: 11734620.
45. Bremer PT, Janda KD. Conjugate Vaccine Immunotherapy for Substance Use Disorder. *Pharmacol Rev.* 2017;69(3):298–315. doi:10.1124/pr.117.013904.
46. Raleigh MD, Baruffaldi F, Peterson SJ, Le Naour M, Harmon TM, Vigliaturo JR, Pentel PR, Pravetoni M. Alters Fentanyl Alters fentanyl distribution and protects against fentanyl-induced effects in mice and rats. *J Pharmacol Exp Ther.* 2019;368(2):282–91. doi:10.1124/jpet.118.253674.

47. Guide for the Care and Use of Laboratory Animals. Washington (DC): National Academies Press (US), National Academy of Sciences; 2011. ISBN-13: 978-0-309-15400-0 ISBN-10: 0-309-15400-6.
48. Torres OB, Antoline JF, Li F, Jalah R, Jacobson AE, Rice KC, Alving CR, Matyas GR. A simple nonradioactive method for the determination of the binding affinities of antibodies induced by hapten bioconjugates for drugs of abuse. *Anal Bioanal Chem.* 2016;408(4):1191–204. doi:10.1007/s00216-015-9223-z.
49. Molecular Operating Environment (MOE), 2019.01; Chemical Computing Group ULC, 1010 Sherbooke St. West, Suite #910, Montreal, QC, Canada, H3A 2R7, 2021; Accessed: March 1, 2021. <https://www.chemcomp.com/>
50. Jalah R, Torres OB, Mayorov AV, Li F, Antoline JF, Jacobson AE, Rice KC, Deschamps JR, Beck Z, Alving CR, et al. Efficacy, but not antibody titer or affinity, of a heroin hapten conjugate vaccine correlates with increasing hapten densities on tetanus toxoid, but not on CRM197 carriers. *Bioconjug Chem.* 2015;26(6):1041–53. doi:10.1021/acs.bioconjchem.5b00085.